J. Appl. Comput. Mech., 5(1) (2019) 103-112
DOI: 10.22055/JACM.2018.25507.1274

ISSN: 2383-4536
jacm.scu.ac.ir

M&MoCS
Shahid Chamran University of Ahvaz

Journal of
Applied and Computational Mechanics

Research Paper

On the Buckling Response of Axially Pressurized Nanotubes Based on a Novel Nonlocal Beam Theory

Mohammad Malikan

Department of Mechanical Engineering, Faculty of Engineering, Islamic Azad University, Mashhad Branch, Iran

Received April 14 2018; Revised May 19 2018; Accepted for publication May 26 2018.
Corresponding author: Mohammad Malikan, mohammad.malikan@yahoo.com

Abstract. In the present study, the buckling analysis of single-walled carbon nanotubes (SWCNT) on the basis of a new refined beam theory is analyzed. The SWCNT is modeled as an elastic beam subjected to unidirectional compressive loads. To achieve this aim, the new proposed beam theory has only one unknown variable which leads to one equation similar to Euler beam theory and is also free from any shear correction factors. The equilibrium equation is formulated by the nonlocal elasticity theory in order to predict small-scale effects. The equation is solved by Navier's approach by which critical buckling loads are obtained for simple boundary conditions. Finally, to approve the results of the new beam theory, some available well-known references are compared.

Keywords: Buckling analysis; Single-walled carbon nanotubes; A new refined beam theory; nonlocal elasticity theory; Navier's approach.

1. Introduction

Carbon nanotubes are the first generation of the nano products discovered in 1991 [1]. The nanotubes are made of twisted graphite sheets with a honeycomb-like structure. These tubes are long and thin and also have high stability and resistance [2]. If the carbon nanotube contains only a rolled graphene, it is called a single-walled carbon nanotube (SWCNT), and if it includes a number of concentric tubes, it is called a multi-walled carbon nanotube (MWCNT) [3-4]. The SWCNT is remarkably strong and hard [5], and is an excellent conductive for the electric current [6-8], which these applications lead to the use of these materials in the electronics industry [9-10]. The carbon nanotube promises a bright future in cellular experiments because they can be used as nano-pipes to distribute very small volumes of fluid or gas into living cells or on surfaces [11-13].

To exploit the industrial amazing properties of nanostructures, it can be highly recommended that the mechanical behavior of them should be analyzed. In the last years, this issue has been taken into consideration by researchers around the world in order to identify the behavior of them under various mechanical conditions. Among these researchers, Malikan et al. [14] published the stability of bi-layer graphene nanoplates subjected to shear and thermal forces on the basis of a medium using numerical solutions. Malikan investigated the stability analysis of a micro sandwich plate with a graphene coating using a refined couple stress theory [15] and the buckling of graphene sheets subjected to nonuniform compression based on a four-variable plate theory using an analytical approach [16]. Yao and Han [17] presented the buckling of double-walled carbon nanotubes by considering thermal influences. They obtained critical buckling loads on the basis of Donnell's equilibrium equation and solved the equation for simply-supported boundary condition. Ansari et al. [18] studied the coupled natural frequency of post stability functionally graded micro/nanobeams on the basis of the strain gradient theory. Wang et al. [19] presented exact modes for post stability characteristics of nonlocal nanobeams in a longitudinal magnetic field. Wang et al. [20] utilized both stress and strain gradient continuum theories to consider the buckling of a nanotube which was embedded in an elastic foundation. Timoshenko beam theory and Navier solution method were employed in their study. They proved that

Published online: January 07 2019

both stress gradient and strain gradient predict the same results if the nonlocal effect is not taken into account. Xiang et al. [21] used the nonlocal elasticity theory for studying the nonlinear free vibration of double-walled carbon nanotubes based on the Timoshenko beam theory. Ansari et al. [22] developed Rayleigh–Ritz method for the buckling of carbon nanotubes considering thermal effects. The classical Donnell shell theory was incorporated in conjunction with the nonlocal elasticity theory of Eringen. Ansari et al. [23] employed Timoshenko beam model to consider the buckling and postbuckling of nanotubes using the nonlocal elasticity theory. The equations were solved using the generalized differential quadrature method along with the pseudo arc-length technique for several boundary conditions. Ansari and Arjangpay [24] presented the meshless local Petrov–Galerkin method to analyze carbon nanotubes under buckling and vibrations conditions. The vibration of thermally post-buckled carbon nanotube-reinforced composite beams resting on elastic foundations was examined by Shen et al. [25]. Beni et al. [26] studied the vibration of shell nanotubes using the nonlocal strain gradient theory and the molecular dynamics simulation. Wang et al. [27] presented the nonlinear vibration of nonlocal carbon nanotubes which were placed on the visco-Pasternak foundation under excitation frequency. Gholami et al. [28] predicted the behavior of post stability of nanotubes subjected to compressive mechanical and thermal loads. They used the nonlinear Euler-Bernoulli beam approach in conjunction with the nonlocal elasticity theory and solved the equations for different boundary conditions. Ansari et al. [29] analyzed the vibration of nanotubes on the basis of the strain gradient and couple stress theories and also molecular dynamic simulation. The generalized differential quadrature technique was applied to convert the differential equations into algebraic ones for several boundary conditions. Some analyses about the dynamic buckling of single and multi-walled carbon nanotubes placed on the elastic substrate with considering thermal stresses were presented by Ansari and Gholami [30] and Gholami et al. [31]. Wave characteristics of conveying fluid for nanotubes modeled as Timoshenko beams was investigated by Gholami et al. [32]. Liu et al. [33] particularly modeled a nanotube conveying fluid in an acoustic environment in order to consider its sound absorption values. Dai et al. [34] analyzed the free vibration and buckling of clamped-free Euler-Bernoulli nanotubes conveying fluid which was exposed to a unidirectional magnetic field. The differential quadrature method (DQM) was employed to solve frequency and buckling equations. In a special case, Ansari and Gholami [35] modeled the dynamic buckling of nanotubes in various boundary conditions on the basis of the nonlocal elasticity theory of Eringen. Yang et al. [36] considered the influences of quantum for free vibration of nanotubes conveying fluid in a thermal environment. The single-walled nanotube was modeled with Euler-Bernoulli beam and the nonlocal elasticity theory was used for considering quantum effects. Jiang and Wang [37] analytically studied natural frequencies of nonlocal Euler beams with considering thermal effects.

In this theoretical study, a new beam theory is reported by reducing the unknown variables from a regenerated shear deformation theory. The SWCNT is modeled as a beam which is subjected to a unidirectional in-plane load. The influence of stress nonlocality is examined by using the nonlocal elasticity theory of Eringen which leads to a size-dependent equation. Furthermore, Navier's technique is exerted to solve the stability equation by assuming simply-supported boundary condition for both ends of the beam.

2. Problem Formulation

Fig. 1 displays a realistic model for a single-walled carbon nanotube subjected to unidirectional compressive loads with length L, outer diameter d, and thickness h parallel to x and z-axes of the right-hand coordinate system, respe ctively. First, according to the first-order shear deformation theory (FSDT), the displacement field at the beam points can be defined as follows [14]:

$$\begin{Bmatrix} U(x,z) \\ V(x,z) \\ W(x,z) \end{Bmatrix} = \begin{Bmatrix} u(x)+z\varphi(x) \\ 0 \\ w(x) \end{Bmatrix} \tag{1a-c}$$

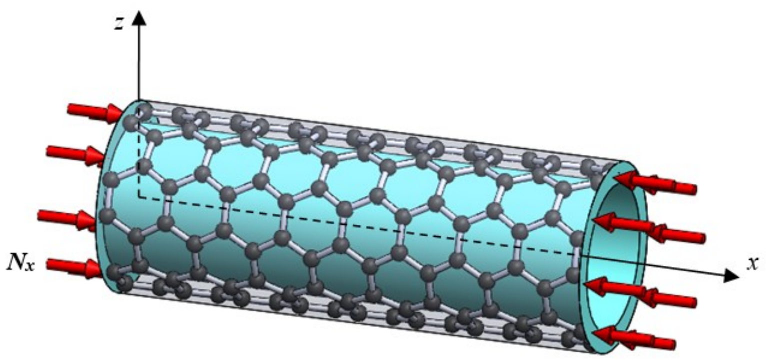

Fig. 1. Schematic picture of the SWCNT subjected to a unidirectional compressive in-plane load

In Eq. (1), the vector quantities of the neutral axis at directions of x and z are u and w, respectively. Furthermore, for defining the swirl of beam elements around the x axis, φ is used. First off, let us reconsider the simple first-order shear deformation theory (S-FSDT) in which it is supposed that the deflection parameter can be re-explained as follows [38-40]:

$$w = w\,(bending) + w\,(shear) \tag{2}$$

On the other hand, the rotation parameter is developed as follows [38-40]:

$$\{\varphi\} = \left\{-\frac{dw_b}{dx}\right\} \tag{3}$$

By replacing Eqs. (2-3) in Eq. (1), the displacement field of the S-FSDT is rewritten [38-40] as:

$$\begin{Bmatrix} U(x,z) \\ W(x,z) \end{Bmatrix} = \begin{Bmatrix} u(x) - z\dfrac{dw_b(x)}{dx} \\ w_b(x) + w_s(x) \end{Bmatrix} \tag{4a-b}$$

Using $w = w_b + w_s$ might not be conceptual; therefore, the S-FSDT is refined as:

$$\begin{Bmatrix} U(x,z) \\ W(x,z) \end{Bmatrix} = \begin{Bmatrix} u(x) - z\dfrac{dw_b(x)}{dx} \\ w_b(x) + W' \end{Bmatrix} \tag{5a-b}$$

Therefore, we can use bending deflection to find the value of w_s as follows:

$$\begin{Bmatrix} \sigma_{xx} \\ \sigma_{xz} \end{Bmatrix} = \begin{Bmatrix} E\,\varepsilon_{xx} \\ 2G\,\gamma_{xz} \end{Bmatrix} \tag{6a-b}$$

After calculating Eq. (6) from Eq. (4), the stresses can be harvested and then by substituting Eq. (6) in Eq. (7), the S-FSDT stress resultants are presented as:

$$\begin{Bmatrix} M_x \\ Q_x \end{Bmatrix} = \int_A \begin{Bmatrix} \sigma_x z \\ \sigma_{xz} \end{Bmatrix} dA \tag{7a-b}$$

Let us use fourth equation of FSDT's governing equations in order to calculate w_s based on w_b:

$$\frac{dM_x}{dx} - Q_x = 0 \tag{8}$$

Now by imposing Eq. (8) into the stress resultants of Eq. (7),

$$EI_c\frac{d^3w_b}{dx^3} - AG\frac{dw_s}{dx} = 0 \tag{9}$$

By integrating from Eq. (9) based on x, simplifying, and then ignoring the integral constant terms, the shear deflection is obtained as follows:

$$w_s = W' = B\frac{d^2w_b}{dx^2} \tag{10}$$

Term B can be explained as:

$$B = \frac{EI_c}{AG},\quad G = \frac{E}{2(1+\upsilon)} \tag{11}$$

where G represents the shear modulus, E is the Young's modulus, I_c $\left(\pi d^4/64\right)$ denotes the moment of area of the cross-section, A is the cross-sectional area, and v is the Poisson's ratio for isotropic nanobeams. Afterwards, the new beam theory is achieved as:

$$\text{Now: } w_b = w \;\; ; \quad \begin{Bmatrix} U(x,z) \\ W(x,z) \end{Bmatrix} = \begin{Bmatrix} u(x) - z\dfrac{dw(x)}{dx} \\ w(x) + B\dfrac{d^2w(x)}{dx^2} \end{Bmatrix} \tag{12a-b}$$

Regarding Hamilton's principle, the potential energy in the whole domain of the beam ($\prod$) is made available and is written in the variational form as follows [41]:

$$\delta\Pi = \int_{t_1}^{t_2} (\delta S + \delta\Omega)dt = 0 \tag{13}$$

In which δS is the variation of strain energy and $\delta\Omega$ is the variation of works, which are done by external forces (Elastic foundations, external forces, etc. which are ignored in this study). The strain energy by variational formulation is calculated as:

$$\delta S = \iiint_v \sigma_{ij}\,\delta\varepsilon_{ij}\,dV = 0 \tag{14}$$

The strain tensor in Eq. (14) is expanded as follows:

$$\begin{Bmatrix} \varepsilon_{xx} \\ \gamma_{xz} \end{Bmatrix} = \begin{Bmatrix} \dfrac{du}{dx} - z\dfrac{d^2w}{dx^2} + \dfrac{1}{2}\left(\dfrac{dw}{dx} + B\dfrac{d^3w}{dx^3}\right)^2 \\ B\dfrac{d^3w}{dx^3} \end{Bmatrix} \tag{15a-b}$$

Therefore, in order to derive the constitutive equations on the basis of the Hamilton's principle, Eq. (16) is shown as follows:

$$\delta S = \iiint_v \left(\sigma_{xx}\,\delta\varepsilon_{xx} + \sigma_{xz}\,\delta\varepsilon_{xz}\right)dV = 0 \tag{16a}$$

$$\delta S = \iiint_v \left(\sigma_{xx}\,\delta\left[-z\frac{d^2w}{dx^2} + \frac{1}{2}\left(\frac{dw}{dx} + B\frac{d^3w}{dx^3}\right)^2\right] + \sigma_{xz}\,\delta\left[B\frac{d^3w}{dx^3}\right]\right)dV = 0 \tag{16b}$$

$$\delta S = \iiint_v \left(\sigma_{xx}\left[-z\frac{d^2}{dx^2}\delta w + \frac{dw}{dx}\frac{d}{dx}\delta w + B^2\frac{d^3w}{dx^3}\frac{d^3}{dx^3}\delta w + B\frac{dw}{dx}\frac{d^3}{dx^3}\delta w + B\frac{d^3w}{dx^3}\frac{d}{dx}\delta w\right] + \sigma_{xz}B\frac{d^3}{dx^3}\delta w\right)dV = 0 \tag{16c}$$

$$\delta S = \iiint_v \left(\begin{aligned} &\frac{d^2}{dx^2}\left(-\sigma_{xx}z\,\delta w\right) + \frac{d}{dx}\left(\sigma_{xx}\frac{dw}{dx}\delta w\right) + \frac{d^3}{dx^3}\left(\sigma_{xx}B^2\frac{d^3w}{dx^3}\delta w\right) + \frac{d^3}{dx^3}\left(\sigma_{xx}B\frac{dw}{dx}\delta w\right) \\ &+ \frac{d}{dx}\left(\sigma_{xx}B\frac{d^3w}{dx^3}\delta w\right) + \frac{d^3}{dx^3}\left(\sigma_{xz}B\,\delta w\right) \end{aligned}\right)dV = 0 \tag{16d}$$

Now, integrating the integrals by parts yields:

$$\delta S = \iiint_v \left(\begin{aligned} &\frac{d^2}{dx^2}\left(-\sigma_{xx}z\,\delta w\right) = -z\frac{d^2\sigma_{xx}}{dx^2}\delta w - z\,\sigma_{xx}\frac{d^2}{dx^2}\delta w \\ &\frac{d}{dx}\left(\sigma_{xx}\frac{dw}{dx}\delta w\right) = \sigma_{xx}\frac{d^2w}{dx^2}\delta w + \frac{d\sigma_{xx}}{dx}\frac{dw}{dx}\delta w + \sigma_{xx}\frac{dw}{dx}\frac{d}{dx}\delta w \\ &\frac{d^3}{dx^3}\left(\sigma_{xx}B^2\frac{d^3w}{dx^3}\delta w\right) = B^2\frac{d^3\sigma_{xx}}{dx^3}\frac{d^3w}{dx^3}\delta w + \sigma_{xx}B^2\frac{d^6w}{dx^6}\delta w + \sigma_{xx}B^2\frac{d^3w}{dx^3}\frac{d^3}{dx^3}\delta w \\ &\frac{d^3}{dx^3}\left(\sigma_{xx}B\frac{dw}{dx}\delta w\right) = B\frac{d^3\sigma_{xx}}{dx^3}\frac{dw}{dx}\delta w + \sigma_{xx}B\frac{d^4w}{dx^4}\delta w + \sigma_{xx}B\frac{dw}{dx}\frac{d^3}{dx^3}\delta w \\ &\frac{d}{dx}\left(\sigma_{xx}B\frac{d^3w}{dx^3}\delta w\right) = B\frac{d\sigma_{xx}}{dx}\frac{d^3w}{dx^3}\delta w + \sigma_{xx}B\frac{d^4w}{dx^4}\delta w + \sigma_{xx}B\frac{d^3w}{dx^3}\frac{d}{dx}\delta w \\ &\frac{d^3}{dx^3}\left(\sigma_{xz}B\,\delta w\right) = B\frac{d^3\sigma_{xz}}{dx^3}\delta w + \sigma_{xz}B\frac{d^3}{dx^3}\delta w \end{aligned}\right)dV = 0 \tag{17}$$

As it can be observed, the last terms in the expressions of Eq. (17) are equal to the expressions of Eq. (16c). Therefore, we get:

$$\delta S=\int_0^L\int_{-h/2}^{h/2}\left(\begin{array}{l}-z\,\sigma_{xx}\dfrac{d^2}{dx^2}\delta w=\dfrac{d^2}{dx^2}\left(-\sigma_{xx}z\,\delta w\right)+z\dfrac{d^2\sigma_{xx}}{dx^2}\delta w\\ \sigma_{xx}\dfrac{dw}{dx}\dfrac{d}{dx}\delta w=\dfrac{d}{dx}\left(\sigma_{xx}\dfrac{dw}{dx}\delta w\right)-\sigma_{xx}\dfrac{d^2w}{dx^2}\delta w-\dfrac{d\sigma_{xx}}{dx}\dfrac{dw}{dx}\delta w\\ \sigma_{xx}B^2\dfrac{d^3w}{dx^3}\dfrac{d^3}{dx^3}\delta w=\dfrac{d^3}{dx^3}\left(\sigma_{xx}B^2\dfrac{d^3w}{dx^3}\delta w\right)-B^2\dfrac{d^3\sigma_{xx}}{dx^3}\dfrac{d^3w}{dx^3}\delta w-\sigma_{xx}B^2\dfrac{d^6w}{dx^6}\delta w\\ \sigma_{xx}B\dfrac{dw}{dx}\dfrac{d^3}{dx^3}\delta w=\dfrac{d^3}{dx^3}\left(\sigma_{xx}B\dfrac{dw}{dx}\delta w\right)-B\dfrac{d^3\sigma_{xx}}{dx^3}\dfrac{dw}{dx}\delta w-\sigma_{xx}B\dfrac{d^4w}{dx^4}\delta w\\ \sigma_{xx}B\dfrac{d^3w}{dx^3}\dfrac{d}{dx}\delta w=\dfrac{d}{dx}\left(\sigma_{xx}B\dfrac{d^3w}{dx^3}\delta w\right)-B\dfrac{d\sigma_{xx}}{dx}\dfrac{d^3w}{dx^3}\delta w-\sigma_{xx}B\dfrac{d^4w}{dx^4}\delta w\\ \sigma_{xz}B\dfrac{d^3}{dx^3}\delta w=\dfrac{d^3}{dx^3}\left(\sigma_{xz}B\,\delta w\right)-B\dfrac{d^3\sigma_{xz}}{dx^3}\delta w\end{array}\right)dzdx=0;\ dy=1 \tag{18}$$

The stress resultants in local forms are specified by the following relations:

$$\begin{Bmatrix}M_x\\ Q_x\end{Bmatrix}=\int_A\begin{Bmatrix}\sigma_x z\\ \sigma_{xz}\end{Bmatrix}dA \tag{19a-b}$$

Now, by substituting Eq. (15) into Eq. (19), the stress resultants in the displacement field are as follows:

$$\begin{Bmatrix}M_x\\ Q_x\end{Bmatrix}=\begin{Bmatrix}-EI_c\dfrac{d^2w}{dx^2}\\ AGB\dfrac{d^3w}{dx^3}\end{Bmatrix} \tag{20a-b}$$

Using Eq. (18) and (19) and some simplyifing yields:

$$\int_0^L\left(\begin{array}{l}\dfrac{d^2}{dx^2}\left(-M_x\delta w\right)+\dfrac{d}{dx}\left(N_x\dfrac{dw}{dx}\delta w\right)+\dfrac{d^3}{dx^3}\left(N_xB^2\dfrac{d^3w}{dx^3}\delta w\right)+\dfrac{d^3}{dx^3}\left(N_xB\dfrac{dw}{dx}\delta w\right)+\\ \dfrac{d}{dx}\left(N_xB\dfrac{d^3w}{dx^3}\delta w\right)+\dfrac{d^3}{dx^3}\left(Q_xB\,\delta w\right)+\\ \dfrac{d^2M_x}{dx^2}\delta w-\dfrac{dN_{xx}}{dx}\left(\dfrac{dw}{dx}+B\dfrac{d^3w}{dx^3}\right)\delta w-\dfrac{d^3N_x}{dx^3}\left(B\dfrac{dw}{dx}+B^2\dfrac{d^3w}{dx^3}\right)\delta w-\\ N_x\left(B^2\dfrac{d^6w}{dx^6}+2B\dfrac{d^4w}{dx^4}+\dfrac{d^2w}{dx^2}\right)\delta w-B\dfrac{d^3Q_x}{dx^3}\delta w\end{array}\right)dx=0 \tag{21}$$

Therefore, Eq. (21) can be further simplified as follows:

$$\begin{array}{l}\dfrac{d}{dx}\left(-M_x\delta w\right)+N_x\left(\dfrac{dw}{dx}+B\dfrac{d^3w}{dx^3}\right)\delta w+\dfrac{d^2}{dx^2}\left(N_xB^2\dfrac{d^3w}{dx^3}\delta w+N_xB\dfrac{dw}{dx}\delta w\right)+\\ +\dfrac{d^2}{dx^2}\left(Q_xB\,\delta w\right)+\displaystyle\int_0^L\left[\dfrac{d^2M_x}{dx^2}-\dfrac{dN_{xx}}{dx}\left(\dfrac{dw}{dx}+B\dfrac{d^3w}{dx^3}\right)-\dfrac{d^3N_x}{dx^3}\left(\dfrac{dw}{dx}+B\dfrac{d^3w}{dx^3}\right)\right.\\ \left.-N_x\left(B^2\dfrac{d^6w}{dx^6}+2B\dfrac{d^4w}{dx^4}+\dfrac{d^2w}{dx^2}\right)-B\dfrac{d^3Q_x}{dx^3}\right]\delta w dx=0\end{array} \tag{22}$$

Finally, ignoring the terms $\dfrac{dN_{xx}}{dx}$ and $\dfrac{d^3N_x}{dx^3}$ in Eq. (22), the terms in the integral section are the nonlinear governing equation as follows:

$$\frac{d^2M_x}{dx^2}-B\frac{d^3Q_x}{dx^3}-N_x\left(B^2\frac{d^6w}{dx^6}+2B\frac{d^4w}{dx^4}+\frac{d^2w}{dx^2}\right)=q_0 \tag{23}$$

and also the higher-order boundary conditions obtained from variational method (Eq. (22)) are presented as follows:

$$-\frac{dM_x}{dx}+B\frac{d^2Q_x}{dx^2}+N_x\left(B^2\frac{d^5w}{dx^5}+2B\frac{d^3w}{dy^3}+\frac{dw}{dx}\right)=0 \tag{24}$$

In which M_x, Q_x, and N_x are nonlocal stress resultants, respectively and q_0 is the transverse static load which is ignored in this study. Here, the quantity N_x is the resultant with respect to the axial applied compressive in-plane force. According to the nonlocal elasticity theory, the following equation is employed [14, 41]:

$$\left(1-\mu\nabla^2\right)\sigma_{ij}^{NL}=\sigma_{ij}^{L}=C_{ijkl}\,\varepsilon_{kl}\ ;\quad \mu(nm^2)=\left(e_0a\right)^2,\ \nabla^2=\frac{d^2}{dx^2}\quad \textit{(NL: Nonlocal, L: Local)} \tag{25}$$

where μ is the stress nonlocality factor and a is an interior determined length [14]. In order to apply the stress nonlocality on the Eq. (23), the following formulation is obtained:

$$\frac{d^2\left(1-\mu\nabla^2\right)M_x^{NL}}{dx^2}-B\frac{d^3\left(1-\mu\nabla^2\right)Q_x^{NL}}{dx^3}-\left(1-\mu\nabla^2\right)N_x^{NL}\left(B^2\frac{d^6w}{dx^6}+2B\frac{d^4w}{dx^4}+\frac{d^2w}{dx^2}\right)=0 \tag{26a}$$

$$\frac{d^2M_x^L}{dx^2}-B\frac{d^3Q_x^L}{dx^3}-\left(1-\mu\nabla^2\right)N_x^L\left(B^2\frac{d^6w}{dx^6}+2B\frac{d^4w}{dx^4}+\frac{d^2w}{dx^2}\right)=0 \tag{26b}$$

The in-plane compressive force is assumed as follows [41-42]:

$$N_x^L=-P_{Cr} \tag{27}$$

Now, incorporating Eq. (20, 27) and inserting them into Eq. (26b) and also some manipulating, lead to the stability equation of OVFSDT in the displacement field as:

$$EI_c\frac{d^4w}{dx^4}+B^2AG\frac{d^6w}{dx^6}-P_{Cr}\left(B^2\frac{d^6w}{dx^6}+2B\frac{d^4w}{dx^4}+\frac{d^2w}{dx^2}\right)+\mu P_{Cr}\left(B^2\frac{d^8w}{dx^8}+2B\frac{d^6w}{dx^6}+\frac{d^4w}{dx^4}\right)=0 \tag{28}$$

3. Navier's solution method

The Navier analytical solution [42] is considered to implement the simply-supported boundary condition according to Eq. (29).

$$w\left(x,t\right)=\sum_{m=1}^{\infty}W_m\sin\left(\frac{m\pi}{L}x\right)e^{i\omega t} \tag{29a}$$

$$\varphi\left(x,t\right)=\sum_{m=1}^{\infty}\Phi_m\cos\left(\frac{m\pi}{L}x\right)e^{i\omega t} \tag{29b}$$

where m is the half-wave number as a integer one [42], W_m and Φ_m are the unknown terms which should be determined and also ω is the natural frequency in the vibrational analysis. Substituting Eq. (29) into Eq. (28), the algebraic equation is obtained from which the equation of critical buckling load is calculated as follows:

$$P_{Cr}=\frac{EI_c\left(\frac{m\pi}{L}\right)^4-\frac{\left(EI_c\right)^2}{AG}\left(\frac{m\pi}{L}\right)^6}{\left(\frac{EI_c}{AG}\right)^2\left(\frac{m\pi}{L}\right)^6-\frac{2EI_c}{AG}\left(\frac{m\pi}{L}\right)^4+\left(\frac{m\pi}{L}\right)^2+\mu\left(\left(\frac{EI_c}{AG}\right)^2\left(\frac{m\pi}{L}\right)^8-\frac{2EI_c}{AG}\left(\frac{m\pi}{L}\right)^6+\left(\frac{m\pi}{L}\right)^4\right)} \tag{30}$$

4. Numerical results

At first glance, it is required to consider the accuracy of the numerical results originated from the proposed beam theory with other theories. Therefore, as can be seen in Tables 1 and 2, references [43-44] are employed. In [43] a nano rod was based on both Euler (Table 1) and Timoshenko (Table 2) beam theories and the equations were solved by using an explicit analytical method. On the other hand, in ref. [44] Euler nano rod was modeled and a differential transform method was utilized in order to obtain numerical results. In fact, both thin and moderately thick beams are compared and carried out with both ends simple boundaries. It is worth noting that by increasing the length to diameter ratio of the nano rod, the results in both Tables are becoming closer to one another. This means that for thin beams the proposed beam theory makes same predictions with Euler beam theory which is an acceptable conclusion. Because thin beam theories like Euler can predict appropriate results only for thin beams due to lack of considering shear strain influences in such a theory. This strain is fundamentally required for the response of moderately thick beams which is embedded in the proposed theory. It can be seen that for lower values of length to diameter ratio which the rod goes into moderately thick and thick cases, the results of Euler beam theory are in a major difference with the current formulation. Furthermore, increasing the small-scale parameter decreases the gap between the results of the current beam theory and others. From Table 2 which compares the new beam theory with Timoshenko beam, it is observed that the difference is further than the first Table. Note that the shear correction factor used in Timoshenko theory can be a serious defect in light of the approximate quantity of k_s=5/6. Although this value has been applied for moderately thick models, it cannot be an exact value to analyze several cases, in particular nanostructures. But in the proposed beam theory, this extra factor is vanished from the governing equation that leads to further accurate results. Generally, Tables 1 and 2 show the close numerical favorable results between the present theory and others from which the theory can be approved. Although the new theory of beam which is used cannot be a complete theory, by carrying out the errors and refining them, the more appropriate numerical results are obtained.

Table 1. Results of critical buckling load (*nN*) developed from several theories for a rod.
E=1TPa, υ= 0.19, d=1nm, m=1.

L (nm)	P_{Cr} (nN)								
	μ=0 nm^2			μ=1 nm^2			μ=2 nm^2		
	[43], EB*, Explicit	[44], EB, DTM**	Present, Navier	[43]	[44]	Present	[43]	[44]	Present
10	4.8447	4.8447	4.9169	4.4095	4.4095	4.4752	3.4735	3.4735	3.5252
12	3.3644	3.3644	3.3991	3.1486	3.1486	3.181	2.6405	2.6405	2.6677
14	2.4718	2.4718	2.4905	2.3533	2.3533	2.3711	2.0574	2.0574	2.0729
16	1.8925	1.8925	1.9034	1.8222	1.8222	1.8327	1.6396	1.6396	1.6491
18	1.4953	1.4953	1.5021	1.4511	1.4511	1.4577	1.3329	1.3329	1.3389
20	1.2112	1.2112	1.2156	1.182	1.182	1.1864	1.1024	1.1024	1.1064

* Euler beam (EB)
** Differential Transform Method (DTM)

Table 2. Results of critical buckling load (*nN*) developed from several theories for a rod.
E=1TPa, υ= 0.19, d=1nm, m=1.

L (nm)	P_{Cr} (nN)									
	μ=0 nm^2		μ=0.5 nm^2		μ=1 nm^2		μ=1.5 nm^2		μ=2 nm^2	
	[43], TB	Present	[43], TB	Present	[43], TB	Present	[43], TB	Present	[43], TB	Present
10	4.7670	4.9169	4.654	4.7985	4.3450	4.4752	3.9121	4.0234	3.4333	3.5252
12	3.3267	3.3991	3.2713	3.3418	3.1156	3.181	2.8865	2.9449	2.6172	2.6677
14	2.4514	2.4905	2.4212	2.4595	2.3348	2.3711	2.2038	2.237	2.0432	2.0729
16	1.8805	1.9034	1.8626	1.8852	1.8111	1.8327	1.7313	1.7515	1.6306	1.6491
18	1.4878	1.5021	1.4766	1.4907	1.4440	1.4577	1.3928	1.4057	1.3269	1.3389
20	1.2063	1.2156	1.1989	1.2082	1.1773	1.1864	1.1431	1.1517	1.0983	1.1064

* Timoshenko beam (TB), k_s=5/6.

The elastic properties and dimensions amounts of the SWCNT to consider the current formulation are used with regard to Table 3.

Table 3. Mechanical properties of the nanotube [26, 45-49]

SWCNT	Elastic properties
	E=1TPa, v=0.25
	Dimensions
	h=0.34nm, d=0.7nm

In order to investigate the behavior of half-wave numbers, Fig. 2 is taken into consideration when different length to diameter ratios are employed. From the diagram, it can be seen that the increase of half-wave increased the critical buckling loads. These curves are the response of the Navier's solution method in case of ignoring sine series in this technique. These results are magnified by using lower deals of half-waves in Fig. 2. It can be concluded that lower values of half-wave numbers noticeably affect the outcomes of lower-dimension ratios.

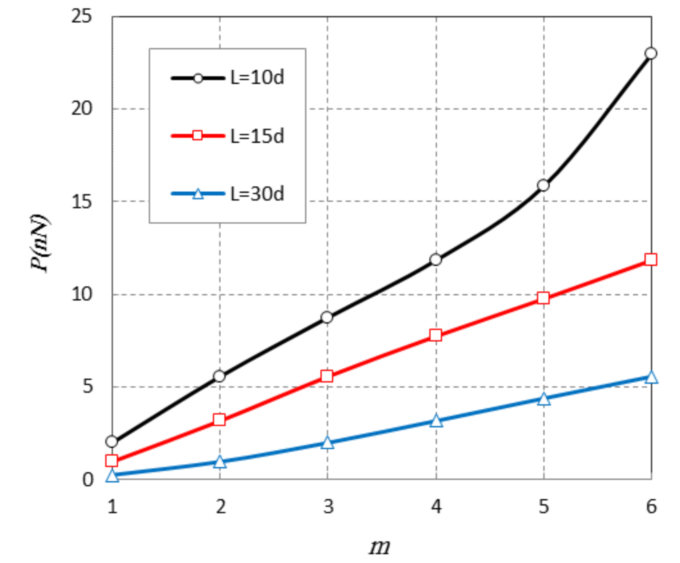

Fig. 2. Several length to diameter ratios versus lower values of half-wave numbers (e_0a=1*nm*)

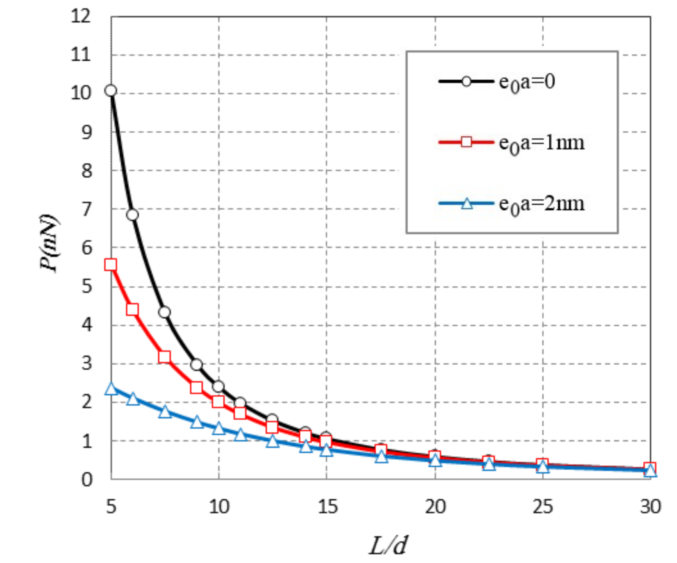

Fig. 3. Nonlocal parameter versus several length to diameter ratios (*m*=1)

The variation of length to diameter ratio is studied in Fig. 3 whilst the nonlocal parameter is chosen differently. It is observed that when the ratio becomes larger, the impact of nonlocal parameter decreased remarkably. In fact, for considerable values of dimension ratio, the critical buckling loads are independent of small-scale influences. This harvest needs further considerations. Therefore, Fig. 4 indicates the growing of nonlocal parameter versus different length to diameter ratios. As can be observed, the critical buckling load decreases regarding various dimension ratios which then lead to same predictions for critical buckling loads. This reducing slope of curves for lower quantities of dimensionless dimensional coefficient is much more than higher ones. From another aspect, it can be seen that in the local case the dimension ratio is an impressive factor. This means that the variation of dimensions in macro conditions is further important than micro ones.

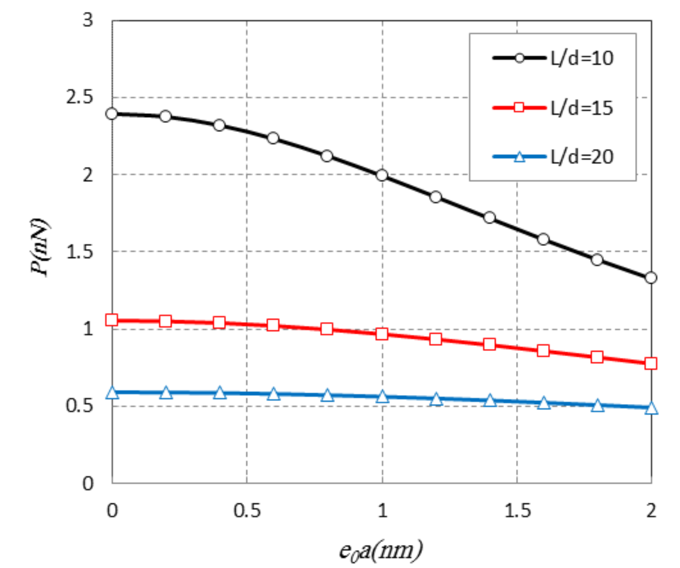

Fig. 4. Different length to diameter ratios versus variations of nonlocal parameter (*m*=1)

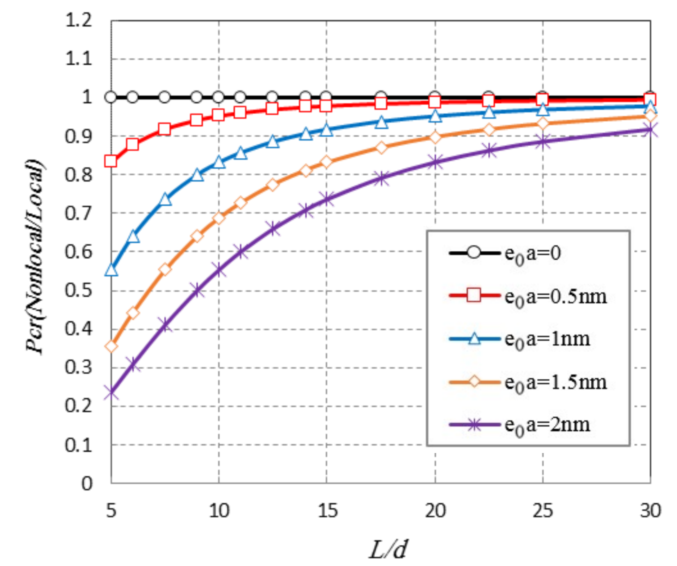

Fig. 5. Nonlocal to local coefficient versus several length to diameter ratios (*m*=1)

Figure 5 considers the ratio of nonlocal to local parameters versus the increase of length to diameter coefficient. According to this figure's results, with an increase in dimension ratio, the quantum effects of the nanotube are decreasing, which can be a reasonable achievement; Because the quantum influences like nonlocality which has been defined by the nonlocal parameter would not be appeared in macro scales. In macro models the results of local and nonlocal analyses are the same as identical values. An urgent necessity to use a small-scale parameter in a nanoscale is shown in Fig. 5.

5. Conclusions

The present study investigated the buckling of single-walled carbon nanotubes subjected to the axial in-plane loads. To achieve this aim, a novel beam theory was formulated to derive the governing equation. The influences of nanoscale were evaluated utilizing the nonlocal elasticity theory of Eringen. Furthermore, Navier's approach was used to calculate the numerical results. The impressive outcomes proved that the Euler beam theory does not include satisfactory results for moderately thick and thick beams. On the other hand, although the Timoshenko beam theory took the impacts of transverse shear strains into account, the used shear correction factor deviated outcomes of this beam approach. The appropriate amount of this factor for nanostructures was not calculated, therefore, the used value could not be appropriate at all. Moreover, the results showed that in the local case, the dimension ratio is an effective factor because the quantum effects do not exist in the macro analysis.

Conflict of Interest

The authors declare no conflict of interest.

References

[1] M. Pacios Pujadó, *Carbon Nanotubes as Platforms for Biosensors with Electrochemical and Electronic Transduction*, Springer Heidelberg, (2012), DOI: 10.1007/978-3-642-31421-6.
[2] F. Liu, R. M. Wagterveld, B. Gebben, M. J. Otto, P. M. Biesheuvel, H. V. M. Hamelers, Carbon nanotube yarns as strong flexible conductive capacitive electrodes, *Colloids and Interface Science Communications*, 3 (2014) 9–12.
[3] Ch. B. Parker, S. A. Raut, B. Brown, B. R. Stoner, J. T. Glass, Three-dimensional arrays of graphenated carbon nanotubes, *Journal of Materials Research*, 27 (2012) 1046–1053.
[4] S. Iijima, Helical microtubules of graphitic carbon, *Nature*, 354 (1991) 56–58.
[5] M.-F.Yu, O. Lourie, M. J. Dyer, K. Moloni, T. F. Kelly, R. S. Ruoff, Strength and Breaking Mechanism of Multiwalled Carbon Nanotubes Under Tensile Load, *Science*, 287 (2000) 637–640.
[6] E. Pop, D. Mann, Q. Wang, K. Goodson, H. Dai, Thermal conductance of an individual single-wall carbon nanotube above room temperature, *Nano Letters*, 6 (2005) 96–100.
[7] S. Sinha, S. Barjami, G. Iannacchione, A. Schwab, G. Muench, Off-axis thermal properties of carbon nanotube films, *Journal of Nanoparticle Research*, 7 (2005) 651–657.
[8] K. K. Koziol, D. Janas, E. Brown, L. Hao, Thermal properties of continuously spun carbon nanotube fibres, *Physica E: Low-dimensional Systems and Nanostructures*, 88 (2017) 104–108.
[9] J. W. Mintmire, B. I. Dunlap, C. T. White, Are Fullerene Tubules Metallic?, *Physical Review Letters*, 68 (1992) 631–634.
[10] X. Lu, Z. Chen, Curved Pi-Conjugation, Aromaticity, and the Related Chemistry of Small Fullerenes (C60) and Single-Walled Carbon Nanotubes, *Chemical Reviews*, 105 (2005) 3643–3696.
[11] T. A. Hilder, J. M. Hill, Modeling the Loading and Unloading of Drugs into Nanotubes, *Small*, 5 (2009) 300–308.
[12] G. Pastorin, Crucial Functionalizations of Carbon Nanotubes for Improved Drug Delivery: A Valuable Option?, *Pharmaceutical Research*, 26 (2009) 746–769.
[13] A. A. Bhirde, V. Patel, J. Gavard, G. Zhang, A. A. Sousa, A. Masedunskas, R. D. Leapman, R. Weigert, J. S. Gutkind, J. F. Rusling, Targeted Killing of Cancer Cells in Vivo and in Vitro with EGF-Directed Carbon Nanotube-Based Drug Delivery, *ACS Nano*, 3 (2009) 307–316.
[14] M. Malikan, M. Jabbarzadeh, Sh. Dastjerdi, Non-linear Static stability of bi-layer carbon nanosheets resting on an elastic matrix under various types of in-plane shearing loads in thermo-elasticity using nonlocal continuum, *Microsystem Technologies*, 23 (2017) 2973-2991.
[15] M. Malikan, Buckling analysis of a micro composite plate with nano coating based on the modified couple stress theory, *Journal of Applied and Computational Mechanics*, 4 (2018) 1–15.
[16] M. Malikan, Analytical predictions for the buckling of a nanoplate subjected to nonuniform compression based on the four-variable plate theory, *Journal of Applied and Computational Mechanics*, 3 (2017) 218–228.
[17] X. Yao, Q. Han, The thermal effect on axially compressed buckling of a double-walled carbon nanotube, *European Journal of Mechanics A/Solids*, 26 (2007) 298–312.
[18] R. Ansari , R. Gholami , M. Faghih Shojaei , V. Mohammadi , M.A. Darabi, Coupled longitudinal-transverse-rotational free vibration of post-buckled functionally graded first-order shear deformable micro- and nano-beams based on the Mindlin′s strain gradient theory, *Applied Mathematical Modelling*, 40(23–24) (2016) 9872-9891.
[19] H. L. Dai , S. Ceballes , A. Abdelkefi , Y. Z. Hong , L. Wang , Exact modes for post-buckling characteristics of nonlocal nanobeams in a longitudinal magnetic field, *Applied Mathematical Modelling*, 55 (2018) 758-775.
[20] B. L. Wang, M. Hoffman, A. B. Yu, Buckling analysis of embedded nanotubes using gradient continuum theory, *Mechanics of Materials*, 45 (2012) 52–60.
[21] L. L. Ke, Y. Xiang, J. Yang, S. Kitipornchai, Nonlinear free vibration of embedded double-walled carbon nanotubes based on nonlocal Timoshenko beam theory, *Computational Materials Science*, 47 (2009) 409–417.
[22] R. Ansari, S. Sahmani, H. Rouhi, Axial buckling analysis of single-walled carbon nanotubes in thermal environments via the Rayleigh–Ritz technique, *Computational Materials Science*, 50 (2011) 3050–3055.
[23] R. Ansari, M. Faghih Shojaei, V. Mohammadi, R. Gholami, H. Rouhi, Buckling and postbuckling of single-walled carbon nanotubes based on a nonlocal Timoshenko beam model, *Z. Angew. Math. Mech.*, 95(9) (2015) 939-951.
[24] R. Ansari, A. Arjangpay, Nanoscale vibration and buckling of single-walled carbon nanotubes using the meshless local Petrov–Galerkin method, *Physica E*, 63 (2014) 283–292.

[25] H.-Sh. Shen, X.-Q. He, D.-Q. Yang, Vibration of thermally postbuckled carbon nanotube-reinforced composite beams resting on elastic foundations, *International Journal of Non-Linear Mechanics*, 91 (2017) 69-75.
[26] F. Mehralian, Y. Tadi Beni, M. Karimi Zeverdejani, Nonlocal strain gradient theory calibration using molecular dynamics simulation based on small scale vibration of nanotubes, *Physica B: Condensed Matter*, 514 (2017) 61-69.
[27] Y.-Z. Wang, Y.-S. Wang, L.-L. Ke, Nonlinear vibration of carbon nanotube embedded in viscous elastic matrix under parametric excitation by nonlocal continuum theory, *Physica E: Low-dimensional Systems and Nanostructures*, 83 (2016) 195-200.
[28] R. Ansari, R. Gholami, S. Sahmani, Prediction of compressive post-buckling behavior of single-walled carbon nanotubes in thermal environments, *Applied Physics A*, 113 (2013) 145-153.
[29] R. Ansari, R. Gholami, S. Ajori, Torsional vibration analysis of carbon nanotubes based on the strain gradient theory and molecular dynamic simulations, *Journal of Vibration and Acoustics*, 135 (2013) 051016.
[30] R. Ansari, R. Gholami, Dynamic stability analysis of embedded single walled carbon nanotubes including thermal effects, *Iranian Journal of Science and Technology, Transactions of Mechanical Engineering*, 39(M1+) (2015) 153.
[31] R. Ansari, R. Gholami, S. Sahmani, A. Norouzzadeh, M. Bazdid-Vahdati, Dynamic stability analysis of embedded multi-walled carbon nanotubes in thermal environment, *Acta Mechanica Solida Sinica*, 28 (2015) 659-667.
[32] R. Ansari, R. Gholami, A. Norouzzadeh, M. A. Darabi, Wave characteristics of nanotubes conveying fluid based on the non-classical Timoshenko beam model incorporating surface energies, *Arabian Journal for Science and Engineering*, 41 (2016) 4359-4369.
[33] Z. J. Zhang, Y. S. Liu, H. L. Zhao, W. Liu, Acoustic nanowave absorption through clustered carbon nanotubes conveying fluid, *Acta Mechanica Solida Sinica*, 29 (2016) 257–270.
[34] L. Wang, Y. Z. Hong, H. L. Dai, Q. Ni, Natural frequency and stability tuning of cantilevered CNTs conveying fluid in magnetic field, *Acta Mechanica Solida Sinica*, 29 (2016) 567–576.
[35] R. Ansari, R. Gholami, Dynamic stability analysis of multi-walled carbon nanotubes with arbitrary boundary conditions based on the nonlocal elasticity theory, *Mechanics of Advanced Materials and Structures*, 24 (2017) 1180-1188.
[36] Y. W. Zhang, L. Zhou, B. Fang, T. Z. Yang, Quantum effects on thermal vibration of single-walled carbon nanotubes conveying fluid, *Acta Mechanica Solida Sinica*, 30 (2017) 550–556.
[37] J. Jiang, L. Wang, Analytical solutions for thermal vibration of nanobeams with elastic boundary conditions, *Acta Mechanica Solida Sinica*, 30 (2017) 474-483.
[38] M. Malikan, Electro-mechanical shear buckling of piezoelectric nanoplate using modified couple stress theory based on simplified first order shear deformation theory, *Applied Mathematical Modelling*, 48 (2017) 196–207.
[39] R. P. Shimpi, Refined Plate Theory and Its Variants, *AIAA Journal*, 40 (2002) 137-146.
[40] M. Malikan, Temperature influences on shear stability a nanosize plate with piezoelectricity effect, *Multidiscipline Modeling in Materials and Structures*, 14 (2017) 125-142.
[41] M. Malikan, M. N. Sadraee Far, (2018), Differential quadrature method for dynamic buckling of graphene sheet coupled by a viscoelastic medium using neperian frequency based on nonlocal elasticity theory, *Journal of Applied and Computational Mechanics*, 4(3) (2018) 147-160.
[42] M. Malikan, V. B. Nguyen, Buckling analysis of piezo-magnetoelectric nanoplates in hygrothermal environment based on a novel one variable plate theory combining with higher-order nonlocal strain gradient theory, *Physica E: Low-dimensional Systems and Nanostructures*, 102 (2018) 8-28.
[43] C. M. Wang, Y. Y. Zhang, S. S. Ramesh, S. Kitipornchai, Buckling analysis of micro- and nano-rods/tubes based on nonlocal Timoshenko beam theory, *Journal of Physics D: Applied Physics*, 39 (2006) 3904-3909.
[44] S. C. Pradhan, G. K. Reddy, Buckling analysis of single walled carbon nanotube on Winkler foundation using nonlocal elasticity theory and DTM, *Computational Materials Science*, 50 (2011) 1052–1056.
[45] E. Ghavanloo, S.A. Fazelzadeh, Vibration characteristics of single-walled carbon nanotubes based on an anisotropic elastic shell model including chirality effect, *Applied Mathematical Modelling*, 36 (2012) 4988-5000.
[46] D. H. Robertson, D. W. Brenner, J. W. Mintmire, Energetics of nanoscale graphitic tubules, *Physical Review B*, 45 (1992) 12592.
[47] A. Benzair, A. Tounsi, A. Besseghier, H. Heireche, N. Moulay, L. Boumia, The thermal effect on vibration of single-walled carbon nanotubes using nonlocal Timoshenko beam theory, *Journal of Physics D: Applied Physics*, 41 (2008) 2254041.
[48] T. Murmu, S. Adhikari, Nonlocal transverse vibration of double-nanobeam-systems, *Journal of Applied Physics*, 108 (2010) 083514.
[49] P. Ponnusamy, A. Amuthalakshmi, Influence of thermal and magnetic field on vibration of double walled carbon nanotubes using nonlocal Timoshenko beam theory, *Procedia Materials Science*, 10 (2015) 243-253.